Collective modes and ultrasonic attenuation in a pseudogapped superconductor

A. V. Shtyk[1,2] and M. V. Feigel'man[3,4]
[1]*Physics Department, Harvard University, USA*
[2]*Moscow Institute of Physics and Technology, Dolgoprudny, Moscow region, Russia*
[3]*L. D. Landau Institute for Theoretical Physics, Chernogolovka, 142432, Moscow region, Russia*
[4]*National Research University "Higher School of Economics," Moscow, Russia*
(Received 13 October 2016; revised manuscript received 1 August 2017; published 24 August 2017)

We develop a theory of collective modes in a model of strongly disordered s-wave superconductor with a localization-induced pseudogap Δ_P, that is much larger than superconducting gap Δ. Then we applied the obtained results to the calculation of the ultrasound decay rate $\alpha(\omega)$ at low-frequencies $\omega \ll k_B T/\hbar$. We show that at low temperatures $T \ll T_c$ the magnitude of the decay rate $\alpha(\omega)$ is controlled by the ratio of T/Δ, while single-particle gap Δ_P does enter the result for $\alpha(\omega)$. Thus, we propose a new method to measure the collective gap Δ in a situation when strong pseudogap is present.

DOI: 10.1103/PhysRevB.96.064523

I. INTRODUCTION

Strongly disordered superconductors near quantum phase transition into an insulator state became again an object of great interest during the past decade, both on the experimental side [1–9] and among theorists [10–13] (references given above are certainly incomplete, due to a large number of papers in the field). On the experimental side, revival of interest in this subject comes about due to new methods that became available. In particular, low-temperature scanning tunneling spectroscopy makes it possible to study properties of superconducting state locally with a nanometer-scale resolution, which allowed demonstration of [1,2] an existence of a strong density-of-states (DoS) suppression at temperatures much above the superconducting transition T_c. In particular, amorphous InO_x films demonstrate virtually zero DoS at and around Fermi level at $T \leqslant 1.5T_c$. Such a phenomenon was called *pseudogap*, in analogy to the somewhat similar phenomenon known for under-doped high-T_c oxide superconductors. Experimentally, clear distinction between single-particle gap (pseudogap) Δ_P and collective superconducting gap Δ was made by means of Andreev contact spectroscopy [14] of the same InO_x films.

Theoretically, it became possible to understand [10] the origin of a pseudogap as a result of an effective (phonon-mediated) electron-electron attraction acting between Anderson-localized electrons. A detailed semiquantitative theory of superconductivity, starting from a BCS-like model with localized single-electron states (near 3D Anderson localization transition) was developed in Ref. [11], elaborating an approach proposed originally in Ref. [15] and developed numerically in Ref. [16]. Qualitatively similar results were later obtained [17–19] by means of renormalization group methods developed for 2D systems. Application of ideas developed in Ref. [11] was found to be useful [20] to the understanding of unusual scaling of superconducting density versus superconducting gap, $\rho_s \propto \Delta^2$, as reported in Ref. [21]. A microwave absorption technique used in Ref. [21] may present an alternative to Andreev spectroscopy [14,22] for measurement of the genuine superconducting gap.

The present paper is devoted to development of a theory of still another phenomenon that is directly related to the collective superconducting gap in disordered materials at very low temperatures near superconductor-insulator transition. Namely, we consider attenuation rate $\alpha(\omega,T)$ of ultrasound wave propagating in a superconducting material with a well-developed pseudogap $\Delta_P \gg \Delta$, at the temperature range $T \ll \Delta/k_B$ and at relatively low frequencies $\hbar\omega \ll k_B T$ (below the Boltzmann's constant k_B is set to unity).

Studies of ultrasound attenuation in disordered metals have long history. Classical mechanism of attenuation was analyzed by Pippard [23] who demonstrated that scattering of electrons by disorder potential leads to weakening of the direct electron-phonon coupling, which suppresses $\alpha(\omega)$. However, Pippard's mechanism is not the only mechanism of inelastic coupling of phonons to the electronic subsystem. As an alternative, one may look for an appropriate version of the Debye-Mandelstam-Leontovich relaxational mechanism of dissipation [24], like Landau-Khlatnikov damping in superconductors discussed, in particular, in Ref. [25]. In Ref. [26] we have shown that ultrasound attenuation rate is intrinsically related to the electron-phonon inelastic energy exchange, which becomes very inefficient at sub-Kelvin temperatures, leading to thermal instabilities and electron overheating [27] in a "neighboring" insulating state of the same (or similar) materials [5,28,29]. We identified in Ref. [26] a few mechanisms leading to (possibly strong) enhancement of the electron-phonon inelastic coupling due to the presence of slowly diffusing modes that may exist in an electronic liquid (particle density, magnetization density, etc.).

In Ref. [30] we have studied one more example of such a diffusion-controlled enhancement, now due to diffusion of thermal energy. This mechanism is quite universally present in any disordered conductor, while its relative strength (with respect to the standard local Pippard mechanism [23]) may vary a lot. In particular, we have calculated [30] ultrasound attenuation $\alpha(\omega,T)$ for both s-wave and d-wave BCS-type superconducting states (as well as in normal doped Silicon); in the s-wave case both Pippard's and diffusion-controlled mechanisms provide an exponentially suppressed low-temperature attenuation $\alpha(\omega,T) \propto \exp(-\Delta/T)$, differing in preexponential factors.

For a pseudogapped superconductor with large single-particle gap Δ_P, all *local* inelastic electron-phonon processes are obviously suppressed $\propto \exp(-\Delta_P/T)$, while ultrasound attenuation due to energy diffusion mode are expected to contain exponential factors $\propto \exp(-\Delta/T)$, with smaller collective gap Δ. Thus, it is natural to expect that low-temperature behavior of $\alpha(\omega,T)$ will be controlled by this latter mechanism. The purpose of the present paper is to calculate $\alpha(\omega,T)$ within the simplest model of a pseudogapped superconductor. Specifically, we will study the attenuation rate of longitudinal ultrasound, since we are interested in the effects related to a collective superconducting mode, while transverse ultrasound is coupled to single-electron modes, which are heavily gapped by large Δ_P. We emphasize, to avoid misintepretation, that pseudogap discussed in the present paper (see Refs. [1–3] for experimental papers and Refs. [10,11,13] for theory) has almost nothing to do with its distant relative known in underdoped copper-oxide superconductors.

The rest of the paper is organized as follows: in Sec. II we formulate our basic model for a superconductor with a large pseudogap and discuss its basic properties; Sec. III is devoted to the derivation of the form of collective modes present in the superconducting state; Sec. IV contains a discussion of the role of long-range Coulomb interaction between electron pairs. In Sec. V we introduce simplest model of electron-phonon coupling relevant for the pseudogapped superconductor. Section VI contains derivation of our main results: ultrasonic attenuation rate $\alpha(\omega,T)$ due to coupling between phonons and collective superconducting amplitude ("Higgs") mode is derived (contribution of the phase mode in the Appendix). Finally, Sec. VII contains our conclusions.

II. MODEL HAMILTONIAN AND EFFECTIVE ACTION

According to the analysis developed in Ref. [11], pseudogapped superconducting state can be realized in poor conductors where single-particle electron states are weakly localized (localization length L_{loc} is larger than mean distance between electrons which eventually participate in superconductivity), and effective Cooper attraction is present between electrons. For the last condition to be realized together with sufficient disorder needed for localization, Coulomb repulsion between conduction electrons should be strongly suppressed. This is the reason to start from the simplest model formulated in terms of "pseudospins" 1/2 introduced originally by Anderson in Ref. [31]:

$$H[\mathbf{S}_i] = -2\sum_{i=1}^{N}\xi_i S_i^z - \frac{1}{2}\sum_{i,j=1}^{N} J_{ij}[S_i^+ S_j^- + S_i^- S_j^+]. \quad (1)$$

Here, $S_i^+ = S_i^x + iS_i^y$ and $S_i^- = S_i^x - iS_i^y$ are operators that create (annihilate) a pair of electrons populating ith localized eigenstate of the free-electron problem, while $S_i^z + 1/2$ counts the number of these pairs. Each localized eigenstate can be characterized by location of its maxima and by its eigenvalue ξ_i. Correspondingly, $2\xi_i$ is a local energy of a Cooper pair siting on a "site" i. For simplicity, we assume sites i to be arranged into cubic lattice with an elementary cell of size a. Hamiltonian Eq. (1) acts in the reduced Hilbert space, spanned by localized electron pairs with zero total spin; single-electron population of any localized state is excluded, due to high extra energy $\Delta_P \gg \Delta$ associated with it (parity gap, see Ref. [32]).

Magnitudes of ξ_i are random with a distribution function $p(\xi)$. We assume a box-shaped $p(\xi) = (2W)^{-1}\Theta(W - |\xi|)$ with energies in the interval $\xi \in (-W,W)$, although any distribution which is flat around Fermi energy position will lead to the same physical results. Then effective density of states (DoS) at the Fermi level is given by $\nu = 1/2Wa^3$. The second term of Eq. (1) describes hopping of Cooper pairs between the orbitals, which is equivalent to interaction between pseudospins. In the long-wavelength limit this (Fourier-transformed) interaction can be expanded in powers of small momenta $\boldsymbol{k}$,

$$J(\boldsymbol{k}) = J[1 - R^2k^2 + O(k^4)], \quad (2)$$

where $J \equiv J(\mathbf{0}) \sim J_{ij} \cdot R^3$ is the overall coupling strength and R can be interpreted as a typical interaction range (i.e., Cooper pair-hopping range). According to Ref. [11], we expect R to be somewhat larger than L_{loc}. The Hamiltonian Eq. (1) does not contain any remnants of long-range Coulomb repulsion between electrons; this is an idealized model which we are going to start from. We will discuss the role of (weak) Coulomb repulsion in the end of the paper. The same Hamiltonian Eq. (1) was employed in Ref. [33] to study quantum phase transition (QPT) between superconducting state (in spin terms, it is the state with nonzero average $\langle S_i^{x,y}\rangle$) and insulating state. In the present paper we will not consider specific features related to this QPT; instead, we are interested in the properties of collective excitations within well-developed superconducting state. This is why we choose to work here with the model of very large interaction (hopping) range $R \gg a$, and we will employ further a mean-field approximation based on this inequility. In this sense, our approach is similar to the usual semiclassical theory of superconductivity.

On a technical side, we choose Fedotov-Popov representation [34] for spin-$\frac{1}{2}$ operators, which is useful to construct a diagrammatic approach and to study collective modes in the ordered state. It is shown in Ref. [34] (see also some extension of this approach in [35]) that exact representation of the partition function for interacting spin systems can be obtained by the representation of spin operators via a special kind of fermionic operators:

$$S_i^\alpha = (1/2)\psi_i^\dagger \sigma^\alpha \psi_i, \quad (3)$$

where σ^α are three Pauli matrices and (anticommuting) two-component spinor operators $\psi(\tau)$, $\psi^\dagger(\tau)$ obey the following boundary condition in the Matsubara imaginary time: $\psi(\tau+\beta) = i\psi(\tau)$, $\psi^\dagger(\tau+\beta) = -i\psi^\dagger(\tau)$, where $\beta = \hbar/T$. Following Ref. [35], we will refer to such a modified fermions as to "semions."

Using representation Eq. (3), we rewrite the original Hamiltonian in the form

$$H = -\sum_i \psi_i^+ \xi_i \sigma^z \psi_i - \tfrac{1}{4}\sum_{i,j} J_{ij}(\psi_i^\dagger \sigma^+ \psi_i)(\psi_j^+ \sigma^- \psi_j). \quad (4)$$

To treat the interaction term, we introduce a complex order parameter field Δ via Hubbard-Stratonovich transformation and integrate out semions. That results in the effective imaginary time action:

$$\mathcal{A}[\Delta] = -\mathrm{Tr}\left[\Delta_i^* J_{ij}^{-1}\Delta_j\right] + \mathrm{Tr}\,\ln\left[i\varepsilon_l + \xi\sigma^z + \tfrac{1}{2}(\Delta^*\sigma^+ + \Delta\sigma^-)\right]. \quad (5)$$

Matsubara energies here are of semionic nature and read as $\varepsilon_l = 2\pi T(l + 1/4)$, while traces go over all spaces.

The equilibrium order parameter is determined by the self-consistency equation that follows from the variation of the action, Eq. (5), over Δ:

$$1 = \frac{J}{2a^3}\int \frac{p(\xi)d\xi}{\sqrt{\xi^2+\Delta^2}} \tanh\frac{\sqrt{\xi^2+\Delta^2}}{T}. \tag{6}$$

This yields $\Delta_0 = 2We^{-1/g}$ for zero-temperature order parameter and $T_c = 2.27We^{-1/g}$ for transition temperature. Here, $g \equiv \frac{J}{2Wa^3}$ is a dimensionless coupling constant.

III. COLLECTIVE MODES: FLUCTUATIONS IN THE ORDERED STATE.

In a superconducting phase, for temperatures $T < T_c$, order parameter can be parametrized as

$$\Delta = (1+\eta)\Delta_0 e^{i\varphi}, \tag{7}$$

revealing two collective modes: a massive (amplitude or Anderson-Higgs) mode η and a massless Goldstone boson, phase ϕ. Below we derive expressions for propagators of both these modes.

The action Eq. (5) can be expanded in fluctuations around the ground state Δ_0. The quadratic Gaussian part describes dynamics of collective modes. Once expanded, the action gives the amplitude propagator,

$$L_\eta^{-1}(\Omega,\boldsymbol{k}) = \frac{\Delta^2}{a^3}[-J^{-1}(\boldsymbol{k}) + \Pi_{xx}(\Omega,\boldsymbol{k})], \tag{8}$$

where Π_{xx} is a σ_x-σ_x semionic correlator (see Fig. 1),

$$\Pi_{xx} = \sum_{\overline{l,\xi}} \mathrm{tr}\,\sigma_x G(i\varepsilon_l)\sigma_x G(i\varepsilon_{l+n}). \tag{9}$$

Here the sign $\sum_{\overline{l,\xi}} T\sum_l \int(d\xi/2W)$ and G is a basic building block of the diagrammatic technique, a semionic Green function that can be represented as

$$G(i\varepsilon_l) = \frac{1}{i\varepsilon_l + \boldsymbol{E}\cdot\boldsymbol{\sigma}} = \sum_\pm \left(\frac{1}{2} \pm \frac{\boldsymbol{E}\cdot\boldsymbol{\sigma}}{2E}\right)\frac{1}{i\varepsilon_l \pm E}, \tag{10}$$

with a vector $\boldsymbol{E} = (\Delta,0,\xi)$, $E = \sqrt{\Delta^2+\xi^2}$.

Calculation of the correlator gives

$$\Pi_{xx} = \sum_{\overline{l,\xi}}\left[\frac{\Delta^2}{E^2}\left(\frac{1}{i\varepsilon_{l+n}-E}\frac{1}{i\varepsilon_l - E} + (E\to -E)\right) + \frac{\xi^2}{E^2}\left(\frac{1}{i\varepsilon_{l+n}+E}\frac{1}{i\varepsilon_l - E} + (E\to -E)\right)\right], \tag{11}$$

where in the low-temperature $T \ll \Delta$ limit the first term gives a negligible exponentially small contribution, while the second term leads to

$$\Pi_{xx} = \int\frac{p(\xi)\xi^2 d\xi}{E^2}\cdot\frac{E}{E^2+(\Omega_n/2)^2}$$
$$= J^{-1} - W^{-1}\frac{\sqrt{4\Delta^2+\Omega_n^2}}{|\Omega_n|}\mathrm{arcsh}\left|\frac{\Omega_n}{2\Delta}\right|, \tag{12}$$

where we made use of the self-consistency Eq. (6). Recalling the gradient expansion Eq. (2) we have an imaginary time amplitude propagator

$$L_\eta^{-1}(i\Omega_n,\boldsymbol{k}) = -\nu\left[\Delta^2 b\left(\frac{i\Omega_n}{2\Delta}\right) + \frac{v^2k^2}{4}\right], \tag{13}$$

where we had introduced a velocity,

$$v = g^{-1/2}\Delta R, \tag{14}$$

and a function,

$$b(ix) = \sqrt{1+x^2}\frac{\mathrm{arcsh}|x|}{|x|}. \tag{15}$$

The obtained propagator has a branch cut along $(-\infty,-2\Delta]\cup[2\Delta,+\infty)$ rather than a simple pole. The analytical continuation to real frequencies $i\Omega_n \to \Omega + i0$ gives for a retarded propagator

$$\left(L_\eta^R(\Omega,\boldsymbol{Q})\right)^{-1} = -\nu\left[\Delta^2 b^R\left(\frac{\Omega+i0}{2\Delta}\right) + \frac{v^2k^2}{4}\right], \tag{16}$$

with a function

$$b^{\mathrm{R}}(x) = \begin{cases}\sqrt{1-x^2}(\arcsin x/x) & |x|<1 \\ \sqrt{1-x^{-2}}\left[\frac{i\pi}{2} + \mathrm{arch}\,x\right] & |x|>1\end{cases}. \tag{17}$$

Note that the gap edge for amplitude excitations is located at the energy 2Δ, unlike usual BCS superconductors where energies of elementary fermionic excitations start from Δ (on the other hand, minimal energy needed to split a Cooper pair is always equal to 2Δ since two quasiparticles should be produced).

For energies just above the gap $b^{\mathrm{R}} \simeq i\pi\sqrt{(x-1)/2}$, so that

$$\left(L_\eta^R(\Omega,\boldsymbol{Q})\right)^{-1} = -\nu\Delta^2\left[i\pi\sqrt{\frac{\Omega-2\Delta}{4\Delta}} + \frac{v^2k^2}{4\Delta^2}\right]$$
$$\times(\Omega > 2\Delta, |\Omega-2\Delta| \ll \Delta), \tag{18}$$

while for large energies $b^{\mathrm{R}} \simeq i\pi/2 + \ln 2x$,

$$\left(L_\eta^R(\Omega,\boldsymbol{Q})\right)^{-1} = -\nu\Delta^2\left[\frac{i\pi}{2} + \ln\frac{\Omega}{\Delta} + \frac{v^2k^2}{4\Delta^2}\right]$$
$$\times(\Omega \gg 2\Delta). \tag{19}$$

Finally, for small energies we have

$$\left(L_\eta^R(\Omega,\boldsymbol{Q})\right)^{-1} = -\nu\Delta^2\left[1 - \frac{\Omega^2}{12\Delta^2} + \frac{v^2k^2}{4\Delta^2}\right]$$
$$\times(|\Omega| \ll 2\Delta), \tag{20}$$

implying a zero-temperature coherence length $\xi = v/2\Delta$.

Meanwhile, phase mode is gapless and relevant energies are well below the gap Δ. In other words we can safely expand the propagator in the frequency Ω_n. Performing

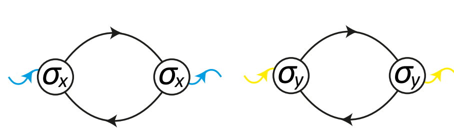

FIG. 1. Self-energy of the collective superconducting mode (amplitude is shown on the left, with blue external lines, and phase is on the right, yellow lines). Black lines stand for semionic propagators.

a straightforward calculation and a subsequent analytical continuation we eventually have

$$\left(L_\phi^R(\Omega,\boldsymbol{k})\right)^{-1} = -\frac{\nu}{4}\left[-\Omega^2 + v^2k^2\right]. \tag{21}$$

Expressions derived in this section for the propagator L_η will be used below in Sec. V for the calculations of the phonon decay rate. In the next section we show that Coulomb interaction gaps out the phase mode by introducing mass term in the propagator L_ϕ. In most real-life scenarios the induced mass is large enough to render the phase mode irrelevant.

IV. ROLE OF COULOMB INTERACTION

In this section we consider modifications caused by the long-range Coulomb interaction that was neglected in the previous sections. The major effect of Coulomb interaction upon the low-temperature symmetry-broken state is formation of the spectral gap Δ_ϕ for the phase mode by the Anderson-Higgs mechanism. We will see that Δ_ϕ is usually large in comparison with the amplitude gap Δ, thus the actual threshold for all inelastic processes at $T = 0$ is determined by Δ.

We consider effectively three-dimensional problem and employ the simplest way to introduce Coulomb interaction between electron pairs:

$$H[\boldsymbol{S}_i] = -2\sum_{i=1}^{N}(\xi_i + \Phi_i)S_i^z - \frac{1}{2}\sum_{i,j=1}^{N} J_{ij}\left[S_i^- S_j^+ + S_i^+ S_j^-\right] + \sum_{i<j}\Phi_i\left(\frac{4\pi e^2}{\epsilon|\boldsymbol{r}_i - \boldsymbol{r}_j|}\right)^{-1}\Phi_j, \tag{22}$$

where in the last term a matrix inversion is implied. Repeating the same steps used above to derive Eq. (5) from Eq. (1), we come now to the action of the following form:

$$\mathcal{A}[\Delta] = -\mathrm{Tr}\left[\Delta_i^* J_{ij}^{-1}\Delta_j\right] + \mathrm{Tr}\,\ln\left[i\varepsilon_l + (\xi+\Phi)\sigma^z + \frac{1}{2}(\Delta\sigma^- + \Delta^*\sigma^+)\right] - \mathrm{Tr}\left[\Phi_i\left(\frac{4\pi e^2}{\epsilon|\boldsymbol{r}_i - \boldsymbol{r}_j|}\right)^{-1}\Phi_j\right]. \tag{23}$$

In the approximation of constant DoS, phase and amplitude modes are decoupled, and the whole effect of Coulomb interaction is to provide a mass to a previously gapless phase mode due to mixing between Φ and $d\phi/dt$. The corresponding part of the action reads

$$\mathcal{A}[\phi,\Phi] = -\nu\Delta^2\mathrm{Tr}\left[\left(-\frac{v^2k^2}{4\Delta^2} + \Pi_{yy}\right)\phi^2 + 2\Pi_{yz}\phi\cdot\left(\frac{\Phi}{\Delta}\right) + \left(\Pi_{zz} + \nu^{-1}V^{-1}(k)\right)\cdot\left(\frac{\Phi}{\Delta}\right)^2\right], \tag{24}$$

where $V(q) = 4\pi e^2/\epsilon q^2$ is Coulomb propagator and semionic polarization functions $\Pi_{\alpha\beta}$, with $\alpha,\beta \in (y,z)$ are defined similar to Eq. (9); calculation of the trace over semionic modes leads to

$$\Pi_{yy}(x) = -\frac{x}{\sqrt{1+x^2}}\mathrm{arcsh}\,x, \tag{25}$$

$$\Pi_{yz}(x) = i\frac{1}{\sqrt{1+x^2}}\mathrm{arcsh}\,x, \tag{26}$$

$$\Pi_{zz}(x) = \frac{1}{x\sqrt{1+x^2}}\mathrm{arcsh}\,x, \tag{27}$$

where $x = \Omega_n/2\Delta$. Next, we integrate out electric potential Φ and obtain the phase-only action in the form

$$\mathcal{A}_{\mathrm{eff}}[\phi] = -\nu\Delta^2\int_\xi \mathrm{Tr}\left[\phi\left(-\frac{v^2k^2}{4\Delta^2} + \Pi_{yy} - \frac{\Pi_{yz}^2}{\Pi_{zz} + \nu^{-1}V^{-1}}\right)\phi\right]. \tag{28}$$

Now we substitute expressions for $\Pi_{\alpha\beta}$ into Eq. (28) and obtain inverse phase propagator in the form

$$L_\phi^{-1}(i\Omega_n) = \frac{\nu v^2k^2}{4}\left[1 + \frac{\epsilon W\Omega_n^2}{4\pi e^2v^2}\left(1 + \left(\frac{\epsilon Wk^2}{4\pi e^2}\right)\frac{\frac{\Omega_n}{2\Delta}\sqrt{1+\left(\frac{\Omega_n}{2\Delta}\right)^2}}{\mathrm{arcsh}\,\frac{\Omega_n}{2\Delta}}\right)^{-1}\right]. \tag{29}$$

This expression should be analytically continued to the real energy axis, $i\Omega_n \to \Omega + i0$, which leads to

$$\left(L_\phi^R(\Omega,k)\right)^{-1} = \frac{\nu v^2k^2}{4}\times\begin{cases} 1 - \frac{\epsilon W\Omega^2}{4\pi e^2v^2}\left(1 + \left(\frac{\epsilon Wk^2}{4\pi e^2}\right)\frac{\frac{\Omega}{2\Delta}\sqrt{1-\left(\frac{\Omega}{2\Delta}\right)^2}}{\arcsin\frac{\Omega}{2\Delta}}\right)^{-1} & \Omega < 2\Delta \\ 1 - \frac{\epsilon W\Omega^2}{4\pi e^2v^2}\left(1 + \left(\frac{\epsilon Wk^2}{4\pi e^2}\right)\frac{\frac{\Omega}{2\Delta}\sqrt{\left(\frac{\Omega}{2\Delta}\right)^2-1}}{\ln\left[\frac{\Omega}{2\Delta}+\sqrt{\left(\frac{\Omega}{2\Delta}\right)^2-1}\right]-i\frac{\pi}{2}}\right)^{-1} & \Omega \geqslant 2\Delta \end{cases}. \tag{30}$$

Propagator of the phase mode Eq. (30) possesses (at $k = 0$) two types of singularities in the complex plane of Ω: a branch cut along $(-\infty,-2\Delta]\cup[2\Delta,+\infty)$ and a simple pole at the plasmon frequency,

$$\Delta_\phi = \sqrt{4\pi e^2\nu v^2/\epsilon}. \tag{31}$$

At small momenta k the pole Eq. (31) shifts according to $\Omega(k) = \sqrt{\Delta_\phi^2 + v_{\phi*}^2k^2}$ and $v_{\phi*} = v\times\frac{\Delta_\phi}{2\Delta}(\ln\frac{\Delta_\phi}{\Delta})^{-1/2}$.

The key point for further analysis is the relation between amplitude gap Δ and plasmon gap Δ_ϕ. For the phase mode to be well-defined at $k > 0$, its energy gap Δ_ϕ should be below 2Δ; otherwise, an imaginary part appears in the inverse propagator Eq. (30) at the mass shell of the massive phase mode. In such a case, actual threshold for all inelastic processes is given by 2Δ and phase mode itself is irrelevant.

Estimates below show that usually $\Delta_\phi \geqslant 2\Delta$ indeed. Instead of using model-dependent relation Eq. (31), we rewrite Δ_ϕ in terms of observables:

$$\Delta_\phi^2 = \frac{4\pi e^2}{\epsilon}\frac{\hbar^2\rho_s}{e^2}, \tag{32}$$

where ρ_s is the superfluid density defined via London relation for supercurrent, $\boldsymbol{j} = -\rho_s \boldsymbol{A}/c$. Next, we use the estimate [20] for superfluid density of pseudogapped superconductor, $\rho_s \sim \nu_0 e^2 R^2 \Delta^2/\hbar^2$, to obtain

$$\frac{\Delta_\phi^2}{4\Delta^2} \approx \frac{\pi e^2}{\epsilon}\nu_0 R^2. \tag{33}$$

Although the model used in Ref. [20] is different from our present one (here we employ a very large interaction range R to use mean-field approximation, while in Ref. [20] hopping of pairs via Mott-type pair resonances was assumed), the results for the ratio Δ_ϕ/Δ are similar in both models.

To get some feeling of relevant numbers, we use parameters known for amorphous superconducting InO_x: for the density of states we take [36] an estimate $\nu_0 \sim 2\cdot 10^{33} \text{erg}^{-1}\text{cm}^{-3}$; for the estimate of effective hopping range R we can use the value of superconducting coherence length $\xi_0 \approx$ 4–5 nm extracted from H_{c2} measurements in less disordered superconducting InO_x in Ref. [37]. Combining all together, we find $\approx 500/\epsilon$ for the right-hand side of Eq.(33). Unfortunately, effective dielectric constant of InO_x in the insulating phase was not yet measured.

Another approach to the problem one can try is a purely theoretical one: consider non-interacting Anderson insulator with a localization length L_{loc} and find its dielectric response at $T = 0$. Such a program was realized recently [38] numerically; for the 3D case it results in $\epsilon \approx 3e^2\nu_0 L_{\text{loc}}^2$. Substituting this estimate into Eq. (33), one finds surprisingly simple and universal result: $\Delta_\phi/2\Delta \approx R/L_{\text{loc}} > 1$. Thus, we conclude that most probably plasmon gap is too large for the phase mode to be relevant for ultrasound decay.

However, the above conclusion can be incorrect for some special highly polarizable materials with a very high intrinsic dielectric constant, like $SrTiO_3$ with its $\epsilon > 10^4$. Very light doping of $SrTiO_3$ makes it superconducting [39,40]. Such a superconductor may have unusually small phason gap $\Delta_\phi \ll \Delta$; in this case the contribution of the phase mode may dominate and we consider this possibility in the Appendix.

V. ELECTRON-PHONON INTERACTION

Interaction between the amplitude mode and longitudinal phonons can be introduced via modulations of the Cooper pair-hopping amplitude (i.e., pseudospin interaction constant) as

$$H_{\text{e-ph}}[\boldsymbol{S}_i] = \kappa \sum_{i,j=1}^{N} (J_{ij}\ \text{div}\boldsymbol{u})[S_i^+ S_j^- + S_i^- S_j^+], \tag{34}$$

with a coupling constant κ that is normally of order of unity, $\kappa \sim 1$. The choice of such a model for e-ph interaction in the effective Hamiltonian makes sense since the pair-hopping term in the Hamiltonian originates from the original phonon-mediated Cooper attraction between electrons.

In general, acoustic wave distorts disorder potential $\sum_i \xi_i S_i^z$ generating electron-phonon interaction terms with a vertex of a large magnitude $\sim W$ [41–43]. However, such terms do not lead to any actual electron-phonon coupling since strong Coulomb interaction maintains electroneutrality and forces electrons to follow the motion of the lattice. That results in suppression of the electron-phonon interaction terms.

To avoid complications related to an explicit account for electroneutrality, we adopt, following Refs. [41,43], the comoving reference frame approach when one considers the reference frame rigidly bound to the lattice. In the reference frame both ions and impurities are stationary and electron-phonon interaction is encoded into modifications of dispersion of electron modes. In weakly disordered conductors this reduces to modification of single-electron dispersion $E_{\text{edge}} + p^2/2m$, where E_{edge} is the edge of the conduction and valence band. In weakly doped semiconductors, the largest coupling constant comes from shifts of this band edge under the lattice strain $\propto E_{\text{edge}}\text{div}\,\boldsymbol{u}$. This vertex is of scalar nature and is screened by Coulomb interaction so that in metals (or strongly doped semiconductors with short Debye screening length) it becomes negligible. This is why subleading momentum-dependent terms have to be included in disordered conductors with large electron densities, eventually yielding the effective vertex of the type $i(p_\alpha v_\beta - [p_F v_F/d]\delta_\alpha\beta)u_\alpha q_\beta$. Notice that after averaging over directions of momentum such a vertex disappears, obeying electroneutrality condition imposed by Coulomb interaction. Following the same idea, we describe electron-phonon interaction by modification of coupling between pseudospins; see Eq. (34).

In a pseudogapped system electric potential is coupled linearly to electron density, which is $\propto S_z$; see Eq. (22). On the contrary, the interaction Eq. (34) corresponds to a nonscalar vertex, coupling phonon to S^+, S^- terms that are orthogonal to S_z, so that there is no scalar part to be eliminated by Coulomb interaction. This is why e-ph interaction Eq. (34) is unaffected by Coulomb interaction.

In a close parallel with electron-phonon interaction in a weakly disordered superconductor, the effect of an acoustic wave within adiabatic approximation in the limit $\omega, q \to 0$ is reduced to modulations of the dimensionless interaction constant,

$$g \to g(1 - \kappa\ \text{div}\boldsymbol{u}). \tag{35}$$

Consecutively, changes of the coupling constant g are most clearly revealed by the change in the ground state Δ_0 due to the exponential sensitivity of the former,

$$\Delta = 2We^{-1/g} \to \Delta\left(1 + \frac{\kappa}{g}\text{div}\boldsymbol{u}\right). \tag{36}$$

Eventually, this gives electron-phonon interaction,

$$\mathcal{A}_{\text{e-ph}}[\Delta, \boldsymbol{u}] = -\text{Tr}\left[\Gamma_\eta \eta^2 \delta\Delta\right], \tag{37}$$

where $\delta\Delta = (\kappa/g)\Delta\text{div}\boldsymbol{u}$ is the change of the order parameter under the lattice strain. In view of the conclusion of the previous section, we focus only on the amplitude mode, the

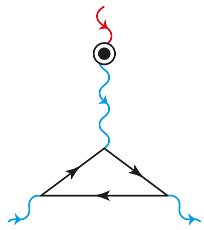

FIG. 2. Interaction vertex of the type phonon-collective-superconducting-mode. This vertex describes the process of conversion of a phonon into two amplitude modes. Black lines in the triangle stand for semionic propagators, red line stands for the phonon and blue line for the amplitude mode.

lowest energy collective mode. The vertex Γ_η is defined by inverse propagator via Ward-like identity (see Fig. 2):

$$\Gamma_\eta = \frac{\delta L_\eta^{-1}}{\delta \Delta}. \tag{38}$$

Using explicit forms of the amplitude Eq. (13) and phase Eq. (21) propagators, one finds the part of action describing electron-phonon interaction:

$$\mathcal{A}_{\text{e-ph}}[\eta,\boldsymbol{u}] = \frac{\kappa_*}{W}\text{Tr}\left[\frac{\partial(\Delta^2 b)}{\partial \ln \Delta}\eta^2 + \frac{v^2}{4}(\nabla\eta)^2\right]\text{div}\boldsymbol{u}, \tag{39}$$

where we had introduced an "enhanced" coupling constant $\kappa_* = \kappa/g$ and $b \equiv b(i\Omega_n/2\Delta)$ is a function given by Eq. (15).

VI. ULTRASONIC ATTENUATION

Ultrasonic attenuation in disordered conductors is usually dominated by electron quasiparticles and proportional to single-particle DoS. The contribution of collective excitations in a typical setup is small either due to strong Coulomb interaction or by symmetry arguments. For example, magnetic field-breaking time-reversal symmetry may activate contribution of spin density fluctuations [26]. Pseudogapped superconductor is yet another example where collective mode contribution to ultrasonic attenuation α dominates over the single-particle contribution due to the presence of a strong gap Δ_P (pseudogap) in the single-particle spectrum that exceeds superconducting gap Δ:

$$\alpha_{\text{collective}} \propto e^{-2\Delta/T} \gg \alpha_{\text{single-particle}} \propto e^{-\Delta_P/T}. \tag{40}$$

This guarantees that collective mode dominates at sufficiently low temperatures.

The ultrasonic attenuation α can be conveniently expressed via an acoustic Q factor,

$$Q^{-1} = \frac{\alpha}{\omega} = \frac{1}{\rho_m\omega^2}\,\text{Im}\,\Sigma_{\text{ph}}^{\text{A}}, \tag{41}$$

where Σ_{ph}^{A} is an advanced phonon self-energy defined on real frequencies. Phonon spectrum is assumed to be acoustic, $\omega(q) = sq$, with sound velocity $s \ll v$, i.e., the phonon propagator reads as

$$D^A(\omega,\boldsymbol{q}) = \frac{1}{\rho_m[(\omega - i0)^2 - s^2\boldsymbol{q}^2] - \Sigma_{\text{ph}}^{A}}. \tag{42}$$

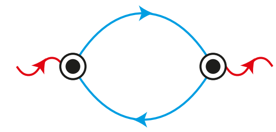

FIG. 3. Ultrasonic attenuation due to collective superconducting mode. This diagram shows contribution of the amplitude mode, when a phonon (red line) falls apart into two amplitude modes (blue lines).

Since ultrasonic frequency $\omega \ll \Delta$ is much smaller than the superconducting gap, acoustic phonon is unable to create a pair of collective excitations. It can, however, interact with already existing thermal excitations. Thus, ultrasonic attenuation is given by processes in which a thermal amplitude mode excitation with energy $\hbar\Omega$ (phase modes are gapped by Coulomb interaction) absorbs an acoustic phonon with energy $\hbar\omega$ and scatters into state with energy $\hbar(\Omega + \omega)$. This process is described by the self energy (see Fig. 3),

$$\Sigma_{\text{ph-}\phi}(i\omega_n,\boldsymbol{q}) = \sum_{m,\boldsymbol{k}} |\Gamma_\phi(\boldsymbol{k},\boldsymbol{q})|^2 \times L_\phi(i\Omega_m,\boldsymbol{k})L_\phi(i\Omega_{m+n},\boldsymbol{k}+\boldsymbol{q}), \tag{43}$$

where the electron phonon interaction vertex Γ_η follows from Eq. (39).

The contribution of amplitude mode η to the phonon decay rate is due to rare (at $T \ll \Delta$) collective excitation with energies close to the threshold $\Omega = 2\Delta$. In this energy region the electron-phonon interaction vertex is singular:

$$\Gamma_\eta(i\Omega_k) \simeq i\kappa_* vq\frac{\Delta^2 b\left(\frac{i\Omega_k}{2\Delta}\right)}{1 + (\Omega_k/2\Delta)^2}, \tag{44}$$

where Ω stands for the energy of collective mode and phonon energy $\omega \to 0$. This singularity comes from the shift of the energy gap position 2Δ induced by phonons via the lattice strain. For real frequencies close to the gap, we obtain for the absolute square of this vertex:

$$|\Gamma_\eta(\Omega)|^2 \simeq \frac{\pi^2}{4}\kappa_*^2 v^2 q^2 \frac{\Delta^5}{|\Omega - 2\Delta|}. \tag{45}$$

If phonon energy ω becomes nonnegligible, the singularity in the vertex Γ is washed out as

$$\frac{1}{\Omega - 2\Delta} \to \frac{1}{\sqrt{(\Omega - 2\Delta)(\Omega + \omega - 2\Delta)}}. \tag{46}$$

Analytical continuation is performed in a standard fashion and gives for the imaginary part of phonon self-energy

$$\text{Im}\,\Sigma_{\text{ph-}\eta}(\omega,\boldsymbol{q}) = \int_{\Omega,\boldsymbol{Q}} |\Gamma_\eta(\Omega,\omega)|^2[B(\Omega+\omega) - B(\Omega)] \times \text{Im}\,L_\eta^{\text{R}}(\Omega,\boldsymbol{k})\,\text{Im}\,L_\eta^{\text{R}}(\Omega+\omega,\boldsymbol{k}+\boldsymbol{q}), \tag{47}$$

where $B(x) = \coth x/2T$ and the propagator of the amplitude mode is given by Eq. (18); in particular, its imaginary part is equal to

$$\text{Im}\,L_\eta^{\text{R}}(\Omega,\boldsymbol{k}) = \frac{4}{v}\frac{\gamma\Delta^2}{\Delta^4\gamma^2 + v^4k^4}, \quad (\gamma = 2\pi\sqrt{(\Omega - 2\Delta)/\Delta}), \tag{48}$$

where it is assumed that $0 < \Omega - 2\Delta \ll \Delta$.

The integral in Eq. (47) has an infrared divergence that is regularized by phonon frequency ω, the leading contribution comes mainly from energies $(\Omega - 2\Delta) \sim \omega$. Finally, for the amplitude contribution to the inverse quality factor, we find

$$Q^{-1}_{\text{ph}-\eta} = \frac{64\sqrt{\pi}}{3}\kappa_*^2 \frac{\Delta^4}{\rho_m s^2 v^3}\left(\frac{\Delta}{T}\right)\left(\frac{\omega}{\Delta}\right)^{3/4} e^{-2\Delta/T}. \quad (49)$$

The result Eq. (49) can be compared to the similar formula from Ref. [30], with ultrasound attenuation in a usual s-wave superconductor leading to $Q^{-1} \propto \exp(-\Delta/T)$. The difference by factor 2 in the exponent is important, and it is due to different statistical weights of excitations in two models: while in BCS theory independent electron and hole quasiparticles appear due to breaking of any Cooper pair, a pseudospin superconductor supports single-particle excitations with the lowest energy 2Δ.

For practical purpose, it is useful to rewrite Eq. (49) in terms of quantities that are more directly measurable. Namely, we employ Eq. (14), which expresses velocity v in terms of Δ, and also note the relation between $\xi_0^2 = R^2/g$ between interaction range R and low-temperature coherence length ξ_0; the result reads

$$Q^{-1}_{\text{ph}-\eta} \approx 40\kappa_*^2 \frac{\Delta}{\rho_m \xi_0^3 s^2}\left(\frac{\Delta}{T}\right)\left(\frac{\omega}{\Delta}\right)^{3/4} e^{-2\Delta/T}, \quad (50)$$

where $\kappa_* \equiv \kappa/g = g^{-1} d\ln\Delta/d\ln n$ is moderately large, due to smallness of $g \approx 1/\ln(E_F/T_c)$. For the estimate of the material-dependent factor $\Delta/\rho_m \xi_0^3 s^2$, we use the parameters of the Indium Oxide [44]: $\rho_m \approx 6$ g/cm^3, $s \approx 3 \times 10^5$ cm/s. With superconducting gap $\Delta \approx 3 \times 10^{-16}$ erg and coherence length [37] $\xi_0 \approx 4 \times 10^{-7}$ cm, we come to the estimate (using also $\kappa_* = 10$):

$$Q^{-1}_{\text{ph}-\eta} \approx 4 \times 10^{-5}\left(\frac{\Delta}{T}\right)\left(\frac{\omega}{\Delta}\right)^{3/4} e^{-2\Delta/T}. \quad (51)$$

With ultrasound frequency $f = \omega/2\pi \sim 10$ GHz and temperatures a few times below Δ, the overall contribution of superconducting electrons to the inverse quality factor of ultrasound is expected to be somewhat below 10^{-6}.

VII. CONCLUSIONS

We have shown in this paper that phonon decay rate in pseudogapped superconductor at low temperatures $T \ll T_c$ is determined by its collective modes. The amplitude mode has a threshold energy $2\Delta < \Delta_P$, so its contribution to the decay of low-frequency phonons is given by Eq. (49). It is proportional to $\exp(-2\Delta/T)$ and dominates over "usual" single-particle contribution which is $\propto \exp(-\Delta_P/T)$. Thus measurements of ultrasound attenuation rate may provide an additional way to determine the value of the collective gap.

If Coulomb interaction between conduction electrons is very strongly suppressed due to high intrinsic dielectric constant $\epsilon \geqslant 10^3$, an additional contribution from the phase mode may be present, see discussion in the Sec. IV and the Appendix.

ACKNOWLEDGMENTS

We are grateful to L. B. Ioffe and V. E. Kravtsov for useful discussions. Research of M.V.F. was partially supported by the Russian Science Foundation Grant No. 14-42-00044. The research was also partially supported by the RF Presidential Grant No. NSh-10129.2016.2.

APPENDIX: ULTRASONIC ATTENUATION DUE TO THE PHASE MODE

As we discussed in the Sec. IV of the main text, Coulomb interaction freezes out phase mode for most realistic scenarios. However, there are some rare exceptions (such as $SrTiO_3$) where the phase mode may remain relevant and dominate ultrasonic attenuation. In this appendix, we consider the case of very weak Coulomb interaction when phason gap can be neglected $\Delta_\phi \approx 0$.

Similar to the amplitude mode, the ultrasonic attenuation due to interaction with the phase mode is given by processes in which acoustic phonon falls apart into two phasons,

$$\Sigma_{\text{ph-}\phi}(i\omega_n,\boldsymbol{q}) = \sum\!\!\!\!\!\!\int_{m,\boldsymbol{k}} |\Gamma_\phi(\boldsymbol{k},\boldsymbol{q})|^2 \times L_\phi(i\Omega_m,\boldsymbol{k}) L_\phi(i\Omega_{m+n},\boldsymbol{k}+\boldsymbol{q}), \quad (A1)$$

where the electron phonon interaction vertex Γ_ϕ follows from Ward-like identity similar to Eq. (38),

$$\Gamma_\phi = \frac{\delta L_\phi^{-1}}{\delta\Delta}. \quad (A2)$$

Using explicit expression for the inverse propagator L_ϕ^{-1},

$$\Gamma_\phi(\boldsymbol{k},\boldsymbol{q}) = iq\frac{\kappa_* \nu v^2}{4}[\boldsymbol{k}\cdot(\boldsymbol{k}+\boldsymbol{q})]. \quad (A3)$$

The main difference with the case of the amplitude mode is the absence of the "mass" term $b(i\Omega_k)$; the contribution of the phase mode will be heavily dominated by infrared region with momenta and frequencies of the phason mode of the order of q, ω, so we had recovered phonon momentum $\boldsymbol{q}$ in the expression for the vertex.

Analytical continuation is performed in a standard fashion and gives for the imaginary part of phonon self-energy

$$\text{Im}\,\Sigma_{\text{ph-}\phi}(\omega,\boldsymbol{q}) = \frac{\kappa_*^2 \nu^2 v^4}{8} q^2 \int_{\Omega,\boldsymbol{Q}} [\boldsymbol{k}\cdot(\boldsymbol{k}+\boldsymbol{q})]^2 \times [B(\Omega+\omega) - B(\Omega)] \times \text{Im}\,L_\phi^{\text{R}}(\Omega,\boldsymbol{k})\,\text{Im}\,L_\phi^{\text{R}}(\Omega+\omega,\boldsymbol{k}+\boldsymbol{q}), \quad (A4)$$

with $B(x) = \coth x/2T$. Since

$$\text{Im}\,L_\phi^{\text{R}}(\Omega,\boldsymbol{k}) = \frac{2\pi}{\nu v k}[\delta(\Omega - vk) - \delta(\Omega + vk)], \quad (A5)$$

as it follows from Eq. (21), we eventually get

$$Q^{-1}_{\text{ph}-\phi} = \frac{2\pi^4 \kappa_*^2}{15}\frac{T^4}{\rho_m s v^4}, \quad (A6)$$

where we had assumed that $\omega(v/s) \ll T$. The result can also be rewritten as

$$Q^{-1}_{\text{ph}-\phi} = \frac{2\pi^4}{15}\kappa^2\left(\frac{a_0}{R}\right)^4\left(\frac{T}{\Delta}\right)^4, \quad (A7)$$

where $a_0 = (\rho_m s)^{-1/4}$ by order of magnitude is equal to a material lattice constant and R is a typical interaction radius.

Comparing the "phason" contribution Eqs. (A6) and (A7) with the contribution of the amplitude mode Eq. (49) from the main text we note that phase and amplitude mechanisms lead to completely different behaviors in function of ultrasound frequency ω and temperature T. In particular, amplitude contribution scales as $\omega^{3/4}$ while the phase one is ω-independent. The ratio of both contributions is given by

$$\frac{Q^{-1}_{\mathrm{ph}-\eta}}{Q^{-1}_{\mathrm{ph}-\phi}} = \underbrace{\frac{480}{\pi^{7/2}}}_{=8.73} \left(\frac{v}{s}\right)\left(\frac{\Delta}{T}\right)^5 \left(\frac{\omega}{\Delta}\right)^{3/4} e^{-2\Delta/T}. \qquad \text{(A8)}$$

Asymptotically, at $T/\Delta \to 0$, phase contribution dominates, although there is a range of relatively small T/Δ, where the main contribution comes from the amplitude mode. Different dependencies of the amplitude and phase contributions to the decay rate on frequency and temperature make it possible to identify both contributions separately. In any case, the result Eq. (A8) is relevant only for rare systems with a weak phason gap $\Delta_\phi \ll \Delta$, such as a lightly doped $SrTiO_3$.

[1] B. Sacépé, Th. Dubouchet, C. Chapelier *et al.*, Nat. Phys. **7**, 239 (2011).
[2] B. Sacépé, C. Chapelier, T. I. Baturina, V. M. Vinokur, M. R. Baklanov, and M. Sanquer, Phys. Rev. Lett. **101**, 157006 (2008).
[3] S. P. Chockalingam, M. Chand, A. Kamlapure, J. Jesudasan, A. Mishra, V. Tripathi, and P. Raychaudhuri, Phys. Rev. B **79**, 094509 (2009).
[4] G. Sambandamurthy, L. W. Engel, A. Johansson, and D. Shahar, Phys. Rev. Lett. **92**, 107005 (2004).
[5] M. Ovadia, B. Sacepe, and D. Shahar, Phys. Rev. Lett. **102**, 176802 (2009).
[6] V. F. Gantmakher and V. T. Dolgopolov, Phys. Usp. **53**, 1 (2010).
[7] A. Goldman and N. Markovic, Phys. Today **51**, 39 (1998).
[8] M. Chand, G. Saraswat, A. Kamlapure, M. Mondal, S. Kumar, J. Jesudasan, V. Bagwe, L. Benfatto, V. Tripathi, and P. Raychaudhuri, Phys. Rev. B **85**, 014508 (2012).
[9] E. F. C. Driessen, P. C. J. J. Coumou, R. R. Tromp, P. J. de Visser, and T. M. Klapwijk, Phys. Rev. Lett. **109**, 107003 (2012).
[10] M. V. Feigel'man, L. B. Ioffe, V. E. Kravtsov, and E. A. Yuzbashyan, Phys. Rev. Lett. **98**, 027001 (2007).
[11] M. V. Feigel'man, L. B. Ioffe, V. E. Kravtsov, and E. Cuevas, Ann. Phys. **325**, 1390 (2010).
[12] G. Lemarie, A. Kamlapure, D. Bucheli, L. Benfatto, J. Lorenzana, G. Seibold, S. C. Ganguli, P. Raychaudhuri, and C. Castellani, Phys. Rev. B **87**, 184509 (2013).
[13] Y. L. Loh, M. Randeria, N. Trivedi, C. C. Chang, and R. Scalettar, Phys. Rev. X **6**, 021029 (2016).
[14] Th. Dubouchet, PhD. thesis, Neel Institute, Grenoble (2010).
[15] M. Ma and P. A. Lee, Phys. Rev. B **32**, 5658 (1985).
[16] A. Ghosal, M. Randeria, and N. Trivedi, Phys. Rev. B **65**, 014501 (2001).
[17] I. S. Burmistrov and I. V. Gornyi, and A. D. Mirlin, Phys. Rev. Lett. **108**, 017002 (2012).
[18] I. S. Burmistrov and I. V. Gornyi, and A. D. Mirlin, Phys. Rev. B **92**, 014506 (2015).
[19] I. S. Burmistrov and I. V. Gornyi, and A. D. Mirlin, Phys. Rev. B **93**, 205432 (2016).
[20] M. V. Feigelman and L. B. Ioffe, Phys. Rev. B **92**, 100509(R) (2015).
[21] D. Sherman, Uwe S. Pracht, B. Gorshunov *et al.*, Nat. Phys. **11**, 188 (2015).
[22] C. Chapelier, invited talk at the Chernogolovka conference 2015, http://intgroup.itp.ac.ru/prog_conf2015.html.
[23] A. B. Pippard, Phil. Mag. **46**, 1104 (1955).
[24] L. D. Landau and E. M. Lifshitz, *Fluid Mechanics* (Pergamon, Oxford, 1977).
[25] K. Miyake and C. M. Varma, Phys. Rev. Lett. **57**, 1627 (1986).
[26] A. V. Shtyk, M. V. Feigelman, and V. E. Kravtsov, Phys. Rev. Lett. **111**, 166603 (2013).
[27] B. L. Altshuler, V. E. Kravtsov, I. V. Lerner, and I. L. Aleiner, Phys. Rev. Lett. **102**, 176803 (2009).
[28] F. Ladieu, M. Sanquer, and J. P. Bouchaud, Phys. Rev. B **53**, 973 (1996).
[29] Tal. Levinson, A. Doron, I. Tamir *et al.*, Phys. Rev. B **94**, 174204 (2016)..
[30] A. V. Shtyk and M. V. Feigelman, Phys. Rev. B **92**, 195101 (2015).
[31] P. W. Anderson, J. Phys. Chem. Solids **11**, 26 (1959).
[32] K. A. Matveev and A. I. Larkin, Phys. Rev. Lett. **78**, 3749 (1997).
[33] M. V. Feigelman, L. B. Ioffe, and M. Mezard, Phys. Rev. B **82**, 184534 (2010).
[34] V. N. Popov and S. A. Fedotov, Sov. Phys. JETP **67**, 535 (1988).
[35] M. N. Kiselev and R. Oppermann, Phys. Rev. Lett. **85**, 5631 (2000).
[36] Zvi Ovadyahu, private communication.
[37] B. Sacépé, J. Seidemann, M. Ovadia, I. Tamir, D. Shahar, C. Chapelier, C. Strunk, and B. A. Piot, Phys. Rev. B **91**, 220508(R) (2015).
[38] M. V. Feigel'man, D. A. Ivanov and E. Cuevas (unpublished).
[39] C. S. Koonce, M. L. Cohen, J. F. Schooley, W. R. Hosler, and E. R. Pfeiffer, Phys. Rev. **163**, 380 (1967).
[40] X. Lin, C. W. Rischau, C. J. vanderBeek, B. Fauque, and K. Behnia, Phys. Rev. B **92**, 174504 (2015).
[41] A. Schmid, Z. Phys. **259**, 421 (1973).
[42] V. I. Yudson and V. E. Kravtsov, Phys. Rev. B **67**, 155310 (2003).
[43] T. Tsuneto, Phys. Rev. **121**, 402 (1960).
[44] T. Wittkowski, J. Jorzick, H. Seitz, B. Schroder, K. Jung, and B. Hillebrands, Thin Solid Films **398–399**, 465 (2001).